Theoretical Analysis of Radial-Axial Ring Rolling Process of 7075 Aluminium Alloy

Jarosław Lulkiewicz[1*], Anna Kawałek[2], Teresa Bajor[2], Maria Gąsiorkiewicz[1], Szymon Szkudelski[1], Michał Chruściński[2], Stanisław Ziółkiewicz[3]

[1] Łukasiewicz Reserch Network – Poznań Institute of Technology, ul. E. Estkowskiego 6, 61-755 Poznań, Poland

[2] Częstochowa University of Technology, ul. J.H. Dąbrowskiego 69, 42-201 Częstochowa, Poland

[3] GFWW Growag Sp. Z o.o. ul. Zdrój 49a, 62-065 Grodzisk Wielkopolski, Poland

* Corresponding author's e-mail: jaroslaw.lulkiewicz@pit.lukasiewicz.gov.pl

ABSTRACT

This paper presents an analysis of the results of the ring rolling process of EN AW-7075 aluminium alloy using numerical modelling. The study of the rheological properties of the AW-7075 aluminium alloy was carried out using the Gleeble 3800 metallurgical process simulator. The modelling of the ring rolling process in the experimental mill was carried out using the Simufact Forming programme based on the finite element method. Based on the analysis of the test results, the speed of the mandrel, the speed of the main roll, the temperature of the metal at the beginning and at the end of the rolling process were determined. The results of research were verified in an experimental mill.

Keywords: aluminium alloy, MES, ring, ring rolling.

INTRODUCTION

The implementation of the forged and rolled ring shaping method was a kind of technological and organizational breakthrough. Compact ring mills made it possible to obtain rings with high geometric accuracy and diameter sizes up to several meters. Currently, as a result of the development of computational and control algorithms, it was possible to launch the world's largest rolling mill for shaping rings with diameters up to 18 meters in China [1]. The production of rings by the rolling method is constantly gaining in importance. The share of the production of rolled rings in the total (by weight) production of forgings is (estimated) in: Europe – 8%, North America (NAFTA countries: USA, Canada, Mexico) – 10%, South America (Brazil) – 6%, and Asia (China and India) – 8%. The weight of roll formed rings in the total production of open-die forgings is 33% in the USA and 68% in Japan [2]. Such a high proportion of rings produced by this method is a direct result of the technological advancement of these countries. It can be concluded that in countries where machinery, equipment and installations are at the highest level of technological advancement, there is a high demand for ring products with uniform structure and mechanical properties [3]. Current development trends in the method of manufacturing forged and rolled rings are towards the reduction of technological allowances of semi-finished products through the design of tools enabling the shaping of rings with profiled inner and outer lateral surfaces [4–9], the manufacture of rings from light alloys [10–13] and composite materials [14–16]. In particular, the second direction of ring-rolling technology development is now being widely explored due to the growing industrial demand for this type of product, particularly in the automotive, aerospace and aviation industries [17].

AIM AND SCOPE OF WORK

The paper presents the results of theoretical research on the rolling process in an experimental

rolling mill of rings made of the EN AW-7075 aluminium alloy. Based on the analysis and the obtained results, a scheme of the relationship between the feed speed of the shaping mandrel and the increase in the diameter of the rolled ring was developed, the fulfilment of which ensures that a constant rolling reduction value per ring revolution is set. The values of the ring forming speed were also determined for the selected aluminium alloy. Experimental verification of the test results was carried out in a model laboratory rolling machine.

Characteristics of material used for the research

The EN AW-7075 aluminium alloy with zinc and magnesium was used for numerical investigations, as it belongs to the alloys which, after appropriate plastic and heat treatment, are characterized by the highest strength among all aluminium alloys.–For the studies, samples taken from round bars with a diameter of 150 mm were used after the extrusion process from the EN AW-7075 aluminium alloy in the T6 state with the chemical composition presented in Table 1.

Knowledge of the characteristics describing the technological properties of the material is the basis for correct numerical simulation of the deformation processes and the design of new or modification of existing technological processes. For plastic working processes, the basic features characterizing the susceptibility of the material to plastic forming are yield stress σ_p and boundary deformation ε_g [18].

Yield stress σp, that is, the stress necessary to initiate and continue the plastic flow of metal under uniaxial stress conditions is a function of strain (ε), strain rate ($\dot{\varepsilon}$), temperature (T) and the history of the deformation course [18].

Determination of the technological plasticity characteristics is particularly difficult for the conditions of hot plastic working because the material structure simultaneously involves processes resulting from the plastic deformation mechanism and the processes of strengthening, as well as thermally activated processes, in addition to time-dependent phenomena leading to weakening of the material [19÷21]. In the available computer

programs intended for solving problems in the field of the plastic flow of metal or for the calculation of forces and deformation force using the finite element method, the values of yield stress σp are determined on the basis of the assumed yield stress function. Most often, yield stress is described by the relationship in the form $\sigma = (\varepsilon, \dot{\varepsilon}, T)$. For the mathematical description of changes in the value of σp depending on strain ε, temperature T and strain rate $\dot{\varepsilon}$, many functions are used, which can be found, among others in works [18, 19, 21, 22÷24].

To describe changes in the value of σp, in the work, a function was adopted that can be transformed into the form of (3). This relationship is often used to determine the σp value in computer programs for the numerical modelling of plastic working processes:

$$\sigma_P = A e^{m_1 T} T^{m_9} \varepsilon^{m_2} e^{\frac{m_4}{\varepsilon}} \cdot \\ \cdot (1 + \varepsilon)^{m_5 T} e^{m_7 - \varepsilon} \dot{\varepsilon}^{m_3} \dot{\varepsilon}^{m_8 T} \text{ [MPa]} \quad (1)$$

where: σ_p – yield stress, T – temperature of the deformed material, ε – actual strain, $\dot{\varepsilon}$ – strain rate, A, m_1 - m_9 – function coefficients.

In the study, the rheological properties of the investigated material were determined on the basis of compression tests performed with a Gleeble 3800 metallurgical simulator, which is in the equipment of the Physical Modelling Laboratory of Metal Forming Processes at the Department of Metal Forming and Safety Engineering at Czestochowa University of Technology. The Gleeble 3800 simulator enables tests to be carried out in a wide temperature range, corresponding to the actual conditions occurring in the analysed technological process. Plastometric tests were carried out for the following parameters:
- temperature: 380 °C, 430 °C, 480 °C
- strain rate: 0.1 s^{-1}, 1 s^{-1}, 10 s^{-1} and 30 s^{-1}
- actual strain: max. 0.9.

The samples were heated at a constant rate of 5 °C/s to the desired temperature, held at this temperature for 20 s, and then deformed. Exemplary, real and approximate courses of changes in the yield stress depending on the actual strain at the temperature of

Table 1. Chemical composition of studied Al alloy, [%]

Al alloy	Si	Fe	Cu	Mn	Mg	Cr	Zn	Ti	Al
7075	0.08	0.15	1.36	0.06	2.38	0.2	5.68	0.03	R

430 °C and a strain rate from 0.01 s^{-1} to 30 s^{-1} for the Al 7075 alloy are shown in Figure 1.

The data presented in Figure 1 shows that during deformation of the Al7075 alloy at low speeds (0.01 s^{-1}, 1 s^{-1}) in the entire examined range of deformations, the material in the initial phase strengthens, however, after reaching the maximum value of plasticizing stress, a plateau effect is observed. On this basis, it can be concluded that under such deformation conditions, a dynamic healing process takes place in aluminium, which eliminates the effects of work hardening. For the samples deformed at the strain rates (1 s^{-1}, 30 s^{-1}), a slight increase in the value of yield stress σ_p is visible on the strengthening curves, then after exceeding the actual strain value of 0.4, a decrease in the stress value is observed.

Analysis of the real curves and approximated strengthening curves shows that the approximation error increases with the temperature of the studied sample, but does not exceed 8%.

It is assumed that the coefficients of the approximating function (3) are sufficiently well selected if the mean approximation error does not exceed 8÷10% [25]. The determined values of the yield stress function coefficients for the Al7075 alloy presented in Table 2 were imported into the program, creating a mathematical reduced of the deformed material.

Model of tools and shaped material

An important element of the research was the determination of the mandrel feed speed (values of the set densities during a single rotation of the ring) and its impact on changes in the shape of the manufactured ring. The engineering modelling program Creo 2.0 was used to model the system of tools - shaping rolls together with their initial position in relation to the charge ring (Fig. 2).

The fully defined shaping system was imported into the numerical program Simufact Forming v.15. The program is equipped with a specialized module for modelling the ring rolling process, in which it is possible to select the appropriate work pattern of tools (rolls) depending on the type of rolling mill used to conduct the rolling process. The kinematic parameters of the device are set by defining the operating modes of individual rolls. For the main roll (1), mandrel (2) and axial rolls (4), a tabular module was used, in which the rotational and linear speeds and directions of their movement were defined. The kinematics of the guide rolls (5) was determined using a special module (KiRAW), in which their position before the start of the process, their movement path and the way they work are determined. The work of the rolls was defined in accordance with the kinematics of the laboratory rolling mill, which
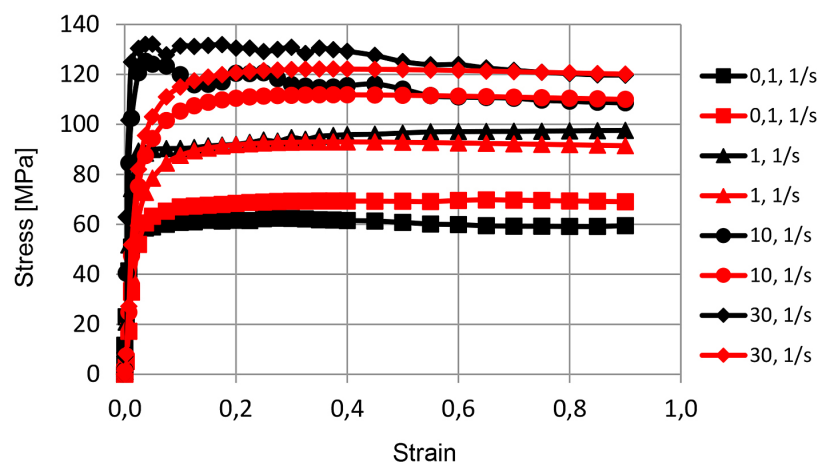

Figure 1. Stress-strain dependence of Al7075 alloy for strain rates in the range 0.01 s-1-30 s1 at 430 °C; black symbols - experimental curves, red symbols - approximate curves

Table 2. Values of parameters A and m$_1$ ÷ m$_9$ used to determine σ_p value of EN AW-7075 alloy

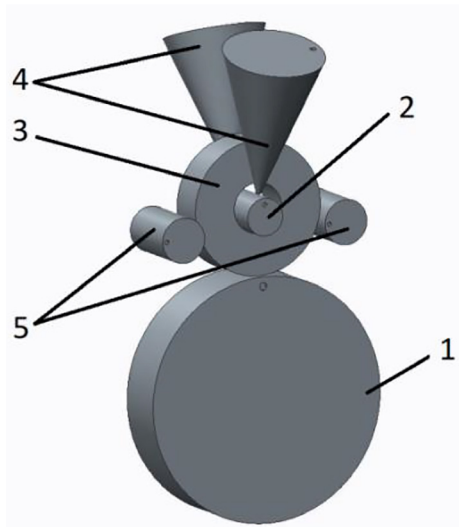| Values of parameters obtained as a result of approximation of Equation 3								
A	*m$_1$*	*m$_2$*	*m$_3$*	*m$_4$*	*m$_5$*	*m$_7$*	*m$_8$*	*m$_9$*
140	-0.0008	0.00034	0.08013	-0.01142	-0.00025	0	0	0

Figure 2. Arrangement of tools during rolling of ring adopted for modelling of the process, made in Creo 2.0 program; 1 – main roll, 2 – mandrel, 3 – ring charge, 4 – axial rolls, 5 – guide rolls

- coefficient of friction: 0.8 for the main roll-ring system,
- coefficient of friction: 0.6 for other rotary drive tools,
- ring charge dimensions:
  - outer diameter: 100 mm
  - inner diameter: 35 mm
  - height: 20 mm
- thermal conductivity coefficient for heat exchange between the deformed rings and rolls 20000 W/m^2K,
- mandrel feed speed:
  - 1 mm/ring revolution
  - 3 mm/ring revolution
- main roll rotational speed: 28 rpm
- rotational speed of axial rolls: passive, resulting from the rotational speed of the shaped ring,
- rotational speed of guide rolls: passive, resulting from the rotational speed of the shaped ring.

Based on the analysis of literature [17, 27] and the technical characteristics of rolling mills, the mandrel feed speed was determined, which was made depending on changes in the rotational speed of the ring. It was assumed that the ring rolling process is carried out by applying a constant rolling reduction for 1 ring revolution. The curve of the linear speed of the mandrel for the value of the set rolling reduction rate during 1 ring revolution was determined with the help of a developed spreadsheet. On the basis of the performed calculations (maintaining the principle of constant volume), two mandrel feed speeds were determined that can be used during the rolling process studies (Fig. 3). Using a spreadsheet, the increments of the outer diameter of the shaped ring over time were calculated, on the basis of which the rotational speed of the axial rolls and their path during rolling were determined. The obtained results were imported in a tabular form into the simulation program, creating kinematic parameters of the tool movements.

was used to carry out the experimental tests. An important element during each simulation is the selection of the shape of the elements and the size of the finite element mesh, which directly affect the duration of calculations and the accuracy of the obtained results. For the investigations, rolling tools were adopted in the form of perfectly rigid elements, while the mesh applied on the surface of the charge was modified using a specialized ring-mesh module. It allows the creation of a mesh of Hexahedral elements arranged angularly on the front surfaces of the charge and circumferentially on the roll surfaces. Such an arrangement and shape of the elements are adapted to the characteristics of the ring rolling process and ensure correct remeshing of the shaped ring during the calculation process. This is confirmed by the results of the research presented in [26], which indicate the highest accuracy of mapping the shape of the ring in the Simufact Forming program in relation to the actual shape obtained by Hexahedral elements.

Selection of kinetic parameters of the rolling process

Numerical modelling of the rolling process of an EN AW-7075 aluminium alloy ring to obtain an outer diameter of Ø150 mm was carried out using the following input parameters:
- charge temperature: 480 °C,
- tool temperature: 150 °C,

ANALYSIS OF RESEARCH RESULTS

Analysis of ring shape changes in rolling process

A properly conducted rolling process should provide a ring with the required diameter (150 mm) and the correct geometrical shape of its wall cross-section. Figure 4 shows the results of numerical tests on the change in
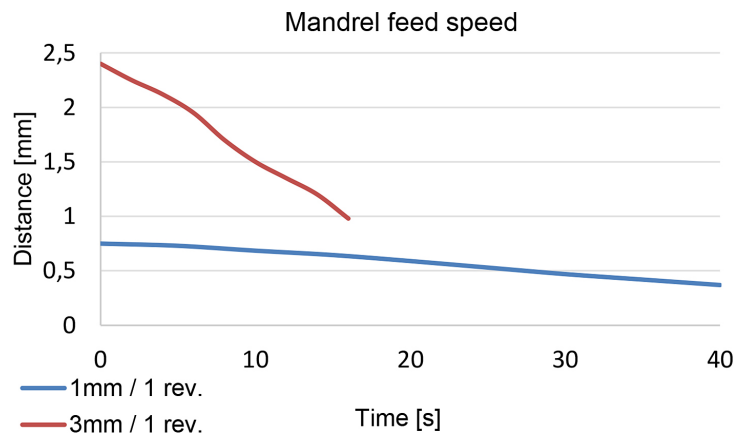
Figure 3. Curve of mandrel feed speed corresponding to rolling reduction of 1 and 3 mm/1 revolution of shaped ring
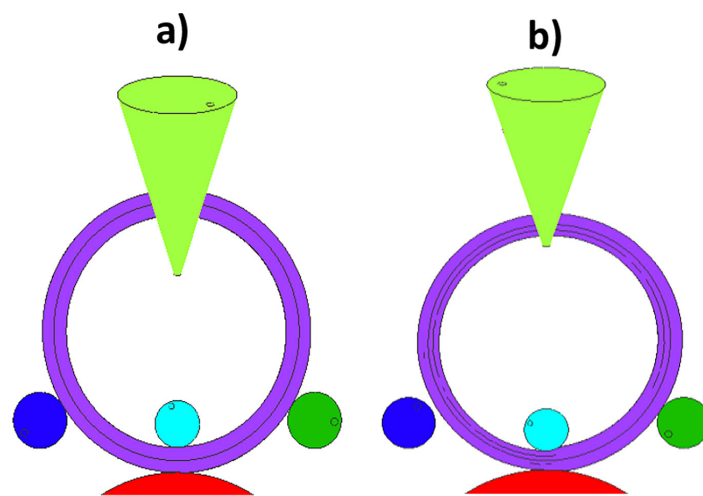

Figure 4. Shape of ring cross-section obtained after rolling process with different densities (mandrel feed speeds): (a) 1 mm/1 ring rev.; (b) 3 mm/1 ring rev.

the geometry of the cross-section of the ring depending on the value of the set rolling reduction during a single rotation of the ring (on the speed of the mandrel feed speed during the rolling process).

The preliminary numerical analysis for the analysed values of the mandrel feed speed of 1 mm/1 ring revolution and 3 mm/1 ring revolution was aimed at verifying the correctness of the adopted parameters of the rolling process. On its basis, it was found that the correct shapes of the rings were obtained for the studied values of the mandrel feed speed. Nevertheless, a more stable course of rolling the ring was noted for the first case, when the speed of the mandrel feed speed was 1 mm/1 revolution of the shaped ring (Fig. 4a). For the second technological case, the deformation process was slightly less unstable and the movement of the ring material in the transverse

direction (sideways) during the shaping process was observed. The correct geometry of the shaped ring with a feed speed of 3 mm/1 revolution was obtained after the process of calibrating its shape.

For both the examined mandrel feed speeds, during the rolling process in the shaped ring, a defect in the form of concavities on the front surfaces, called "fish tail", was formed (Fig. 5). This phenomenon, caused by uneven deformation of the strip along its height, is also observed in real rolling processes, e.g. when rolling thick plates, when too small individual rolling reductions are applied during rough rolling. In the case of industrial ring mills, this disadvantage is eliminated by applying a greater reduction in the wall thickness of the ring during rolling by the axial movement of the axial rolls. During numerical simulations, due to the inability to move the axial rolls in the

laboratory rolling mill, such a reduction in the height of the rolled strip was not applied.

In order to verify the correctness of the developed numerical models of the rolling process, an analysis of changes in the initial volume of the charge and the ring was carried out after completing the calculations, which amounted to 145107 mm^3 and 144593 mm$^{3.}$ The volumes of the charge and the final ring obtained during the numerical investigations differ slightly. The loss of volume between the charge and the shaped ring was 514 mm^3, which is a change of 0.36% of the original volume. The obtained result does not affect the simulation results because the loss of metal volume of 514 mm^3 translates into a loss of 0.04 mm in the thickness of the ring with a diameter of 150 mm.

Analysis of reduced stress distributions in deformed metal

As part of the research, numerical simulations were performed for the mandrel feed speed: 1 mm/1ring rev. and 3 mm/1 ring rev. Figure 6 presents a diagram of the ring cross-section for which the distributions of reduced stress and reduced strain rate in the rolling process were analysed. Figure 7 show the reduced stress distribution in the metal for 50% advancement of the rolling process. Figures 8 show the reduced stress distributions in the metal after 75% advancement of the ring rolling process. Figure 9 show the reduced stress distributions in the metal for the final phase of ring formation.

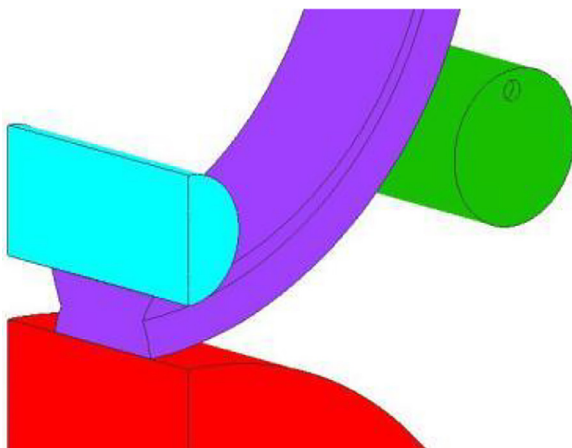Along with the progress of the rolling process (50%), an increase in plasticized zones can
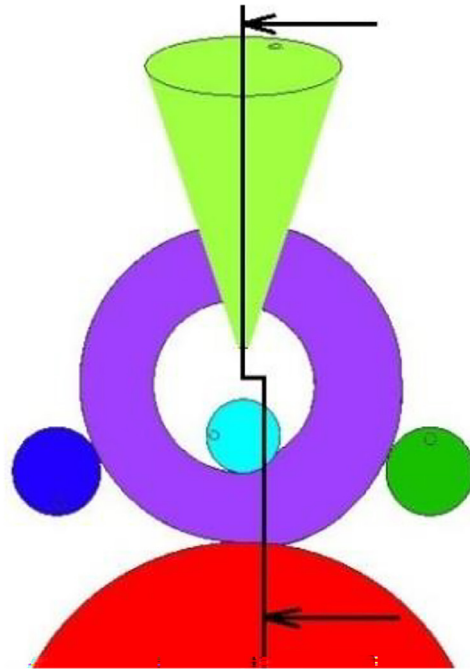

Figure 6. Diagram of ring cross-section for analysis of reduced stress distribution and reduced strain rate in rolling process

be noticed both in the areas of contact with the mandrel and with the main roll. Such a difference in the stress distribution results in faster plastic flow of the material in the axial direction in contact with the tools and limited flow in the middle zone, which causes the formation of concavities on the faces of the shaped ring ("fish tail" defect). It is worth noting that the lower the speed of mandrel movement, the greater the concavity effect on the end face is, which can be explained by the smaller thickness of the plasticized zone at the metal-tool contact surfaces. In the central part of the cross-section of the ring wall, the occurrence of a zone with stress close to the value of the yield stress of the material is still observed (Fig. 7). Only after 75% advancement of the process, in the entire cross-section, did the value of reduced stress exceed 120 MPa and the material was plasticized in the entire cross-section (Fig. 8). At the final stage of the rolling process (100% advancement of the process), the metal exhibits the highest values of post-stress, reaching a value of approx. 170 MPa (Fig. 9).

Based on analysis of the conducted research, it was found that the shape of the concave on the ring faces changes depending on the speed of mandrel movement. At the low mandrel feed speed (1 mm/1 revolution), sharper corners are observed, especially on the main roll side, while
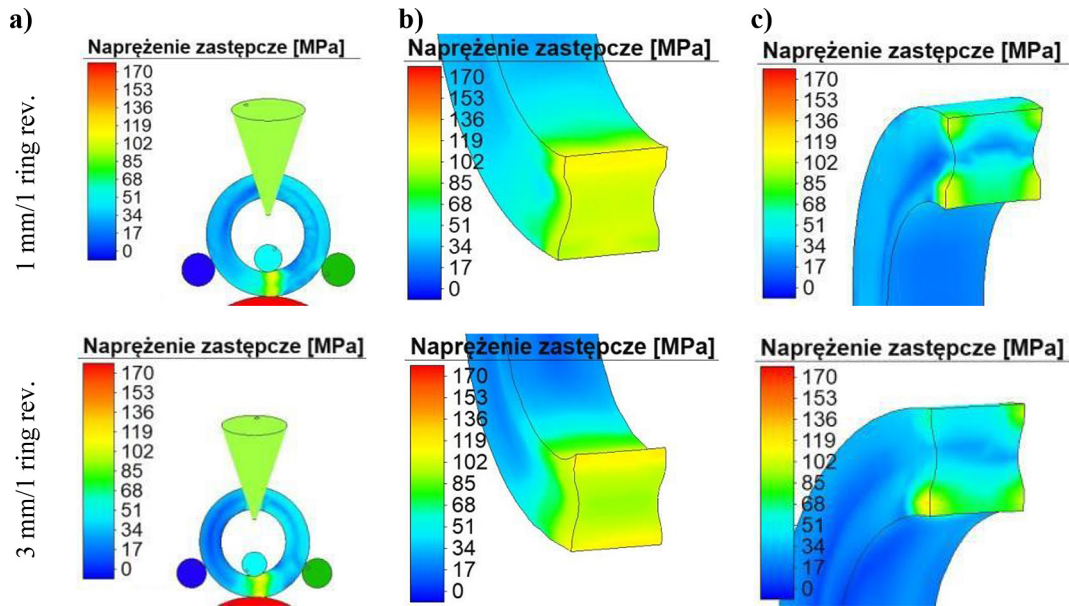

Figure 5. Concavity on faces of rolled ring – "fish tail"

Figure 7. Distribution of reduced stress for 50% advancement of rolling process with absolute indentation of 1 and 3 mm/1 ring revolution; (a) general view of process, (b) cross-section of ring
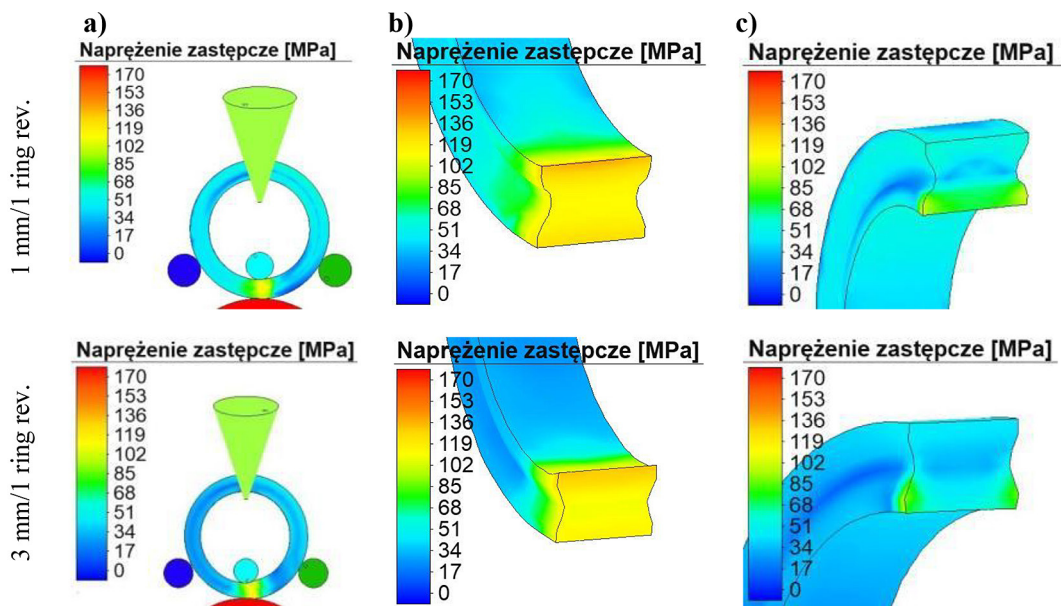

Figure 8. Distribution of reduced stress after 75% advancement of numerical rolling process with absolute indentation of 1 mm/1 ring revolution, (a) general view of process, (b) cross-section of ring shaped with main roll and mandrel, (c) cross-section of ring shaped with axial rolls

at the high mandrel feed speed (3 mm/1 revolution), the face of the ring is flat with a concave groove in the middle parts. When analysing the cross-section of the rings in the axial roll impact zone, it was noticed that in the initial stages of the rolling process, regardless of the mandrel feed speed, the values of reduced stress at the corners locally exceeded 120 MPa, which proves that the metal flows as a result of the pressure of the rolls. Along with the progress of the rolling process,

increasingly more plasticization of the metal in the rolling gap is observed, the plastic flow of the metal in the transverse direction is smaller and less, and thus the effectiveness of the impact of the axial rolls decreases. The reduced stress does not exceed the value of the yield stress of the material. In the final phase of the rolling process, the transverse movement of the metal is low and the axial rolls do not deform the areas of metal at the end face of the ring.
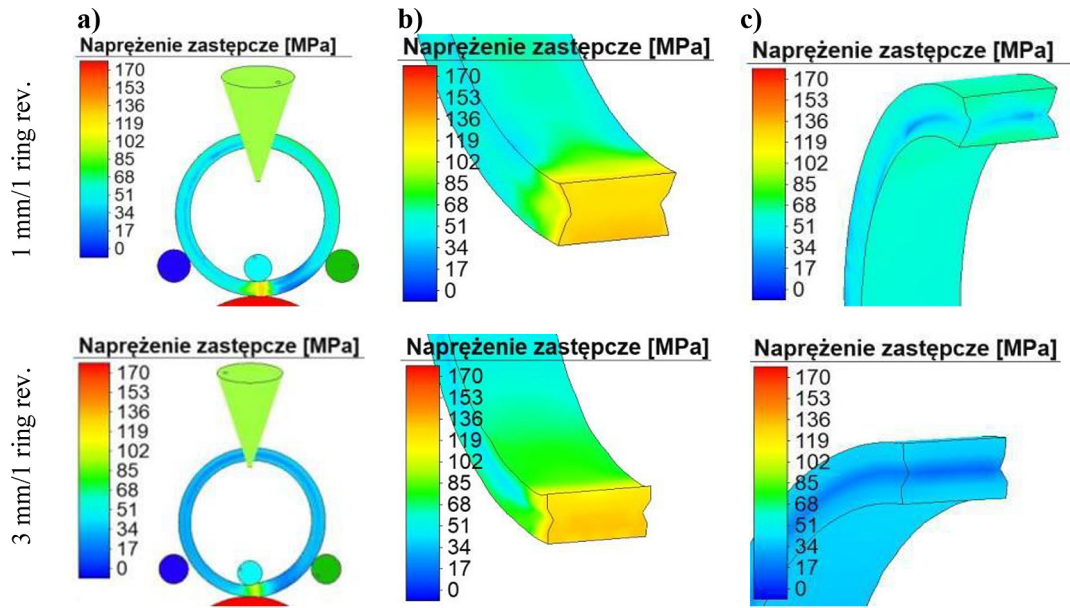
Figure 9. Distribution of reduced stress after 100% advancement of rolling process with absolute indentation of 1 and 3 mm/1 ring revolution, (a) general view of process, (b) cross-section of ring shaped with main roll and mandrel, (c) cross-section of ring shaped with axial rolls
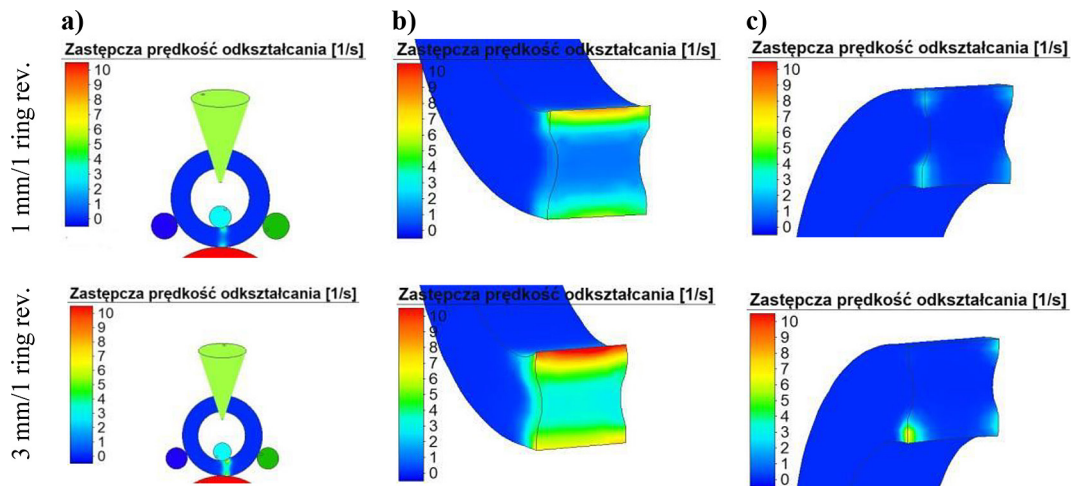

Figure 10. Distribution of reduced strain rate in metal after 50% advancement of rolling process, with absolute indentation of 1 and 3 mm/1 ring revolution, (a) general view of process, (b) cross-section of ring shaped with main roll and mandrel, (c) cross-section of ring shaped with axial rolls

Analysis of reduced strain rate fields in deformed metal

Figure 10 show the results for 50% advancement of the process. Figure 11 show the study results for 75% advancement of the rolling process. Figure 12 show the distributions of the reduced strain rate in the metal after a full rotation of the ring (after 100% advancement of the rolling process). In the middle of the rolling process (50% of the process duration), for the analysed mandrel feed speeds, a decrease in the central zone on the cross-section of the deformed metal can be observed, in which the reduced strain rate is close to zero (Fig. 10), while in the final phase of the process (advancement above 75%), the reduced strain rate in the entire cross-section is greater than the value of 2 s^{-1} (Fig. 12). For the highest value of the mandrel feed speed, it is in the range from 10 to 4 s^{-1} and it varies in the cross-section from the surface of the mandrel to the surface of the main roll. In the zone of impact of the axial rolls on the metal, the minimum values of the reduced strain rate are observed. The results of the analysis of changes in the value of
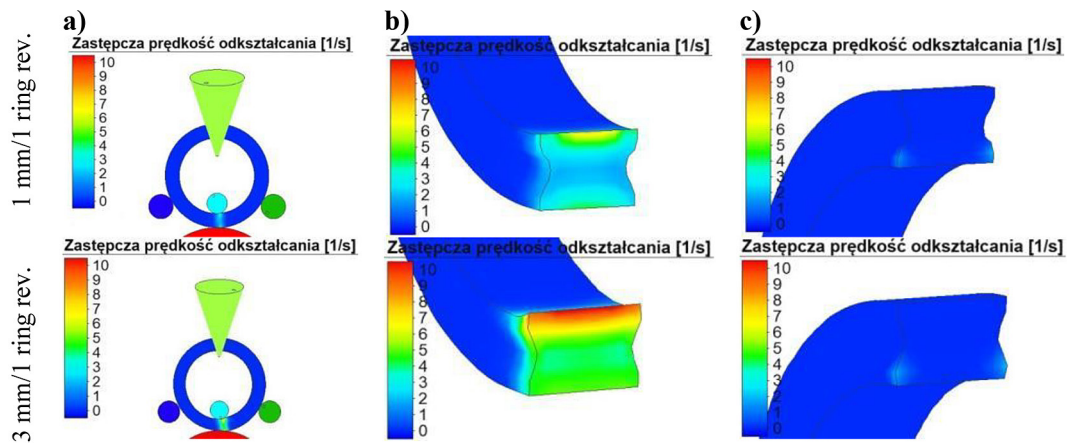
Figure 11. Distribution of reduced strain rate in metal after 75% advancement of rolling process, with absolute deformation of 1 and 3 mm/1 ring revolution, (a) general view of process, (b) cross-section of ring shaped with main roll and mandrel, (c) cross-section of ring shaped with axial rolls
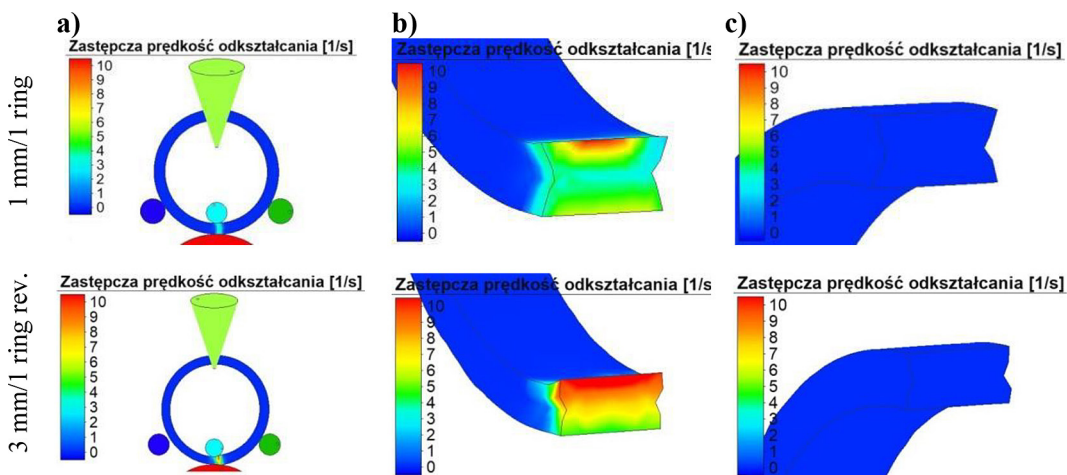

Figure 12. Distribution of reduced strain rate in metal after 100% advancement of rolling process, with absolute deformation of 1 and 3 mm/1 ring revolution; (a) general view of process, (b) cross-section of ring shaped with main roll and mandrel, (c) cross-section of ring shaped with axial rolls

the reduced strain rate were confirmed by the results obtained on the basis of the analysis of changes in the value of reduced stress in the metal during the rolling process.

Analysis of temperature distribution in rolled ring

Figure 13 show changes in the metal temperature during the rolling of rings for all the studied mandrel feed speeds. Based on the analysis of the temperature changes in the deformed ring during the rolling process, it can be concluded that in none of the considered technological cases did excessive cooling of the shaped ring occur. Using the mandrel feed speed of 1 mm /1 revolution of the shaped ring,

the temperature of the ring at the end of rolling was 382 °C. After increasing the mandrel feed speed to the value of 3 mm/1 revolution of the shaped ring, the temperature value in the final phase of the rolling process was 441 °C. Based on the analysis of the research results, it can be concluded that for low speeds of mandrel movement, the ring temperature in the final stage of the process will be close to the lower limit of the recommended shaping temperature for the examined alloy. In the case of a speed greater than 3 mm/1 revolution of the shaped ring, the rolling process takes place under almost isothermal conditions, which would be advantageous when forming rings with a high degree of plastic processing under industrial conditions.
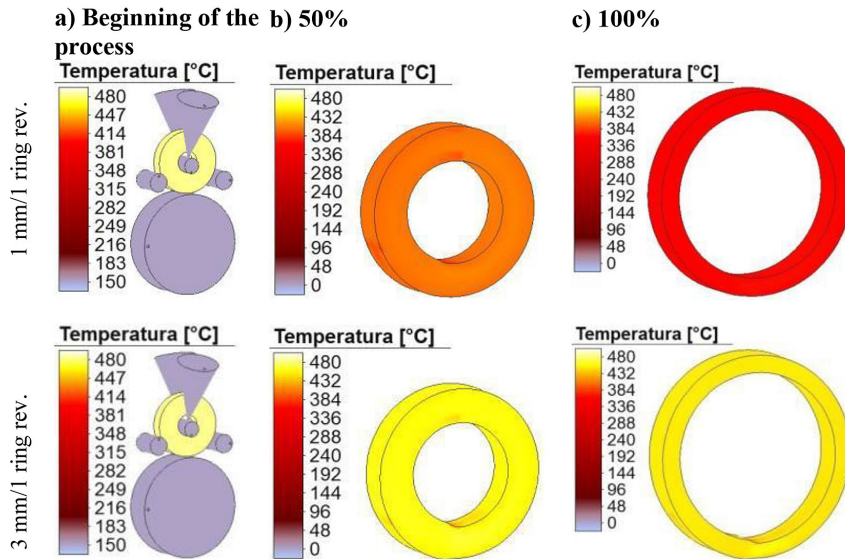
**a) Beginning of the b) 50%
process**

c) 100%

Figure 13. Change in ring temperature during rolling process for mandrel feed
speed1and 3 mm/1 ring revolution, at various stages of deformation process

Analysis of changes in energy and force parameters of rolling process

Determining the power and energy parameters of the rolling process is important due to the specific, allowable pressure of the deformed metal on the working tools and the maximum allowable power of the mill drives for forming the rings. The basic and most important parameter of the ring rolling process is the total metal pressing force exerted on the moving mandrel. It is that which determines the minimum requirements for the mill drive. A too high value of metal pressure on the mandrel during the ring shaping process may result in changes to the design of the rolling mill or a change in the rolling technology consisting in reducing unit rolling reductions and re-performing numerical simulations of the rolling process. Figures 14 and 15 show the courses of changes in the metal pressure

on the mill mandrel during deformation of the metal, for the values of the mandrel feed speed during one rotation of the ring adopted for the analysis. On the basis of the studies carried out to determine the value of the metal pressure force on the mill mandrel, it was found that the maximum value of the force needed to roll an EN AW-7075 aluminium alloy ring is:

- for a mandrel speed of 1 mm/revolution: 23.5 kN,
- for a mandrel speed of 3 mm/revolution: 30.4 kN.

In the initial phase of the ring rolling process, an increase in the value of the mandrel pressure was observed until plastic flow of the shaped ring was observed, followed by stabilization of the force value. The lowest force value was obtained for the mandrel feed speed equal to 1 mm/ 1 revolution. After an increase in force in the first phase of the rolling process, a plateau effect was observed, followed by a
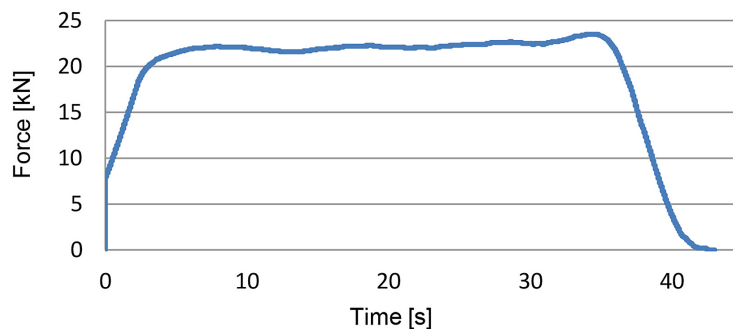

Figure 14. Course of changes in metal pressure force on mill mandrel during
ring rolling with mandrel feed speed 1 mm/1 ring revolution
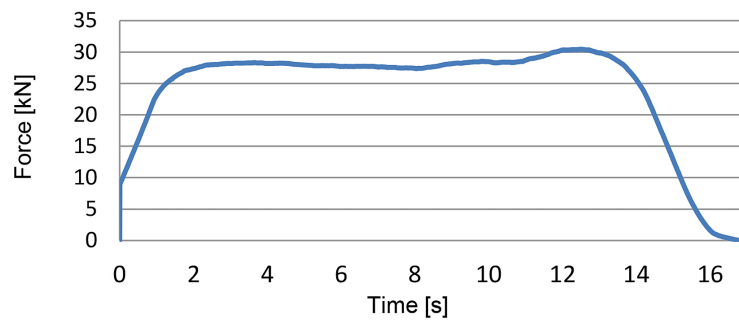
Figure 15. Course of curve of mandrel pressure force during ring rolling with mandrel feed speed 3 mm/1 ring rotation

decrease in force in the last phase of the rolling process. For the mandrel feed speed equal to 3 mm/1 revolution, a greater increase in the pressure force on the mandrel was observed. In the final phase of the rolling process, there was also a decrease in the force value. This is the phase in which the ring shape is calibrated – 4 revolutions of the ring with the rolls at their end positions. For the implementation of laboratory tests, the feed speed of the mandrel was selected: 1 mm/1ring revolution.

LABORATORY STUDIES

In order to experimentally verify the results of the numerical studies at Lukasiewicz- Poznan Institute of Technology, the laboratory rolling machine was designed, shown in Figure 16. The model laboratory rolling machine was designed as a work cage placed on the body of an existing research device owned by the Mechanical Engineering Research Group, Lukasiewicz - Poznan Institute of Technology. The adoption of such a solution was aimed at reducing the financial outlay for the construction of the testing device. This represented certain design limitations that directly affected the limitations of research capabilities. The model device does not fully reflect the kinematics of industrial rolling mills, but allows to illustrate the rolling process. Industrial rolling mills are equipped with complex control systems for the drive units of rollers and rollers, which allow to control the course of the forming process in real time, based on complex algorithms.

Rolling was carried out on the test device in accordance with the shaping parameters that were adopted in the numerical tests. Below, Figure 17 shows the translation rings made on the rolling machine. The obtained samples of rolled rings, regardless of the rolling parameters adopted, had a defect in the form of a concavity on the faces of the so-called "fish tail" (Fig. 18). The reason for the formation of concavity on the face is the
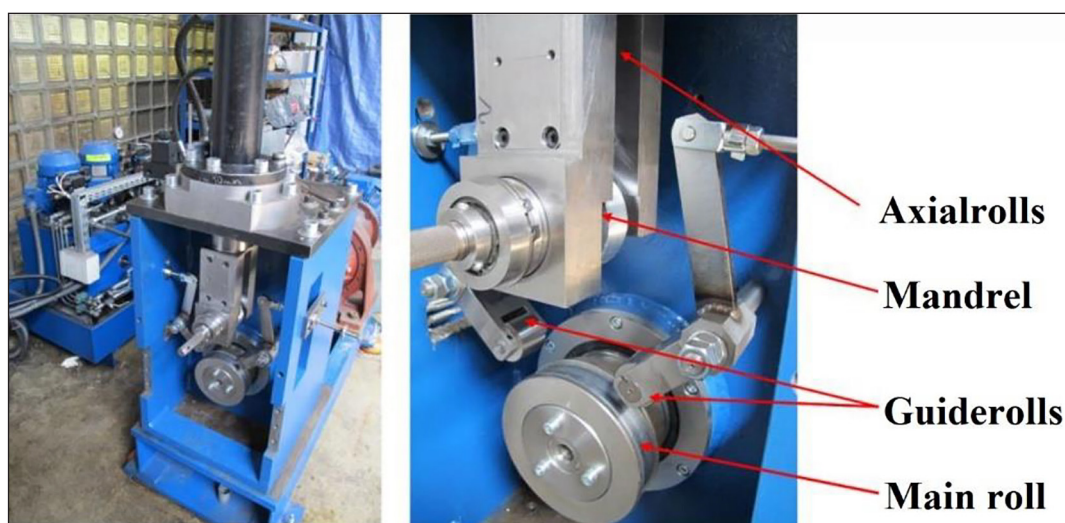

Figure 16. Laboratory rolling machine

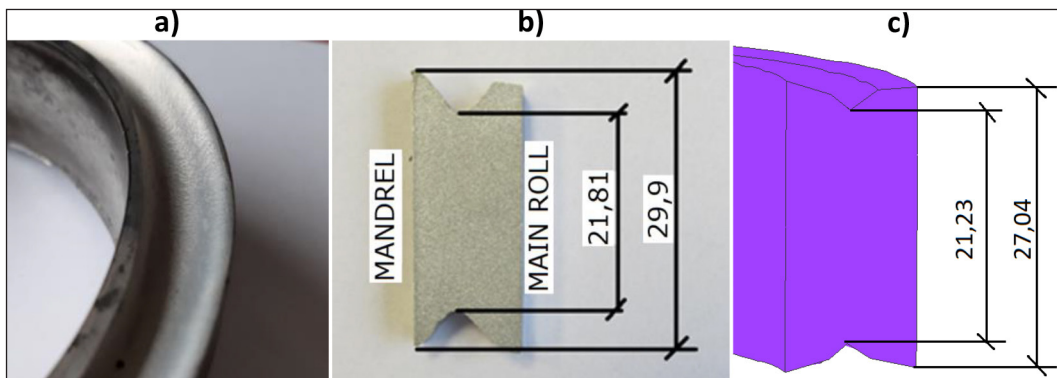**Figure 17.** Example rings made on the experimental rolling mill

Figure 18. "Fish tail" on the faces of the ring: (a) obtained in laboratory tests,
(b) dimensions on the cross-section of the ring obtained in laboratory tests,
(c) dimensions on the cross-section of the ring obtained in simulation tests

inability to move the conical rollers in the laboratory rolling mill to compensate for the uneven flow of metal in the roll-gap. It should be noted that the results of numerical tests indicated the occurrence of this defect during model rolling processes. The thickness of the ring measured at the bottom of the grooves on the faces (fish tail) obtained in laboratory tests has a similar value to the ring obtained in simulation tests. In the case of the ring rolling process without displacement of conical rollers, it is necessary to use a blank with a height equal to the final product. The example plot of the metal pressure force on the mandrel during the rolling process under laboratory conditions had a similar course to the mandrel pressure force plots obtained by numerical simulations in Simufact Forming v. 15 software (Fig. 19). The difference between the value of the pressure force in the actual process and the value of this force obtained in the theoretical tests
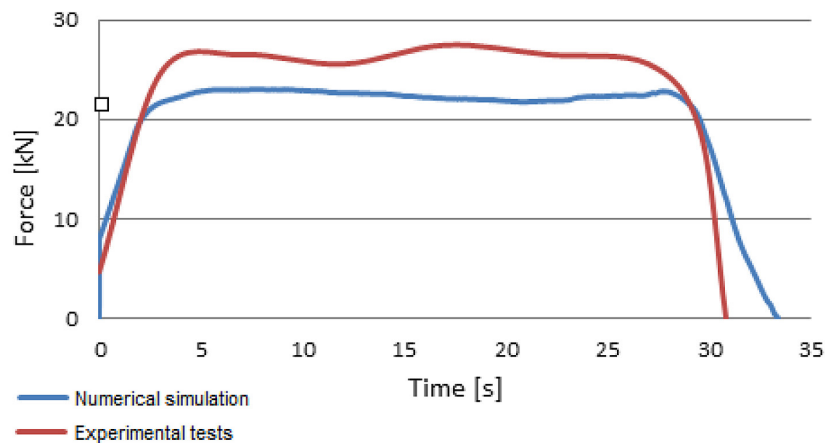
Figure 19. Comparison of the course of the metal pressure force on the mandrel obtained during numerical simulation of the rolling process with the force recorded during experimental tests, corrected for the resistance force

averaged 3.2 kN, which is 14.5%. Such a difference is acceptable, as the error is less than 15%, which is widely recognized as a correct result in engineering calculations.

CONCLUSIONS

Based on the theoretical research carried out on the rolling process of EN AW-7075 aluminium alloy rings, it was found that it is possible to carry out such a process under real conditions. The strain rates adopted for the plastometric tests were correct, which was demonstrated during numerical simulations of the ring rolling process. The computer program Simufact Forming v. 15 for the numerical simulation of the ring rolling process, ensured reflection of the kinematics of the experimental rolling mill operation and the carrying out of the rolling process with the different values of mandrel feed speed. The control studies conducted on the compliance with the law of constant volume showed that the loss of ring volume after the rolling process, in relation to the charge mass, is relatively small and amounts to about 0.04%, which did not significantly affect the results of the numerical calculations and can be neglected. Based on the obtained results of the numerical investigations, it was found that:

- when rolling rings from a selected alloy, it is possible to use a mandrel feed speed in the range of 1 mm/1 revolution÷3 mm/1 ring revolution. The use of speeds in this range ensures that the correct shape of the ring is obtained, while maintaining the other parameters of the rolling process at the level of permissible values.

- it is also possible to determine the value of forces and the possibility of potential rolling defects.

The results of the numerical studies were confirmed during experimental tests. The specified speed of the mandrel displacement adopted in the experimental studies proved to be correct and ensured that the rolling process was carried out correctly and the rings with the correct shape were obtained. There was a concave ("fish tail") defect on the faces of the rings. The force values were similar to those obtained by numerical modeling. The differences in the values of forces obtained in theoretical and experimental studies did not exceed 15%, which can be considered sufficient accuracy in engineering issues.

Acknowledgements

REFERENCES

1. Bogdhan M. New world record for seamlessly rolled rings, SMS Group Magazine, Mönchengladbach, November 2018.

2. Euroforge data presented at an international conference in Berlin in 2014.

3. Lulkiewicz J., Kawałek A., Pachutko B., Bajor T., Szkudelski S. Microstructure and mechanical properties of forged and rolled rings made from X20Cr13 steel, Metalurgija 2023, 62(3–4), 379–382.

4. Lee K.H., Ko D.C., Kim D.H., Lee S.B., Sung N.M., Kim B.M. Design method for intermediate roll in multi-stage profile ring rolling process: The case for excavator idler rim, International Journal of Precision Engineering and Manufacturing 2014, 15(3): 503–512, DOI:10.1007/s12541-014-0364-3

5. Arthington M.R., Havinga J., Duncan S.R. Control of ring rolling with variable thickness and curvature. International Journal of Material Forming 2020, 13: 161–175.

6. Cleaver Ch.J., Arthington M.R., Mortazavi S., Allwood J.M. Ring rolling with variable wall thickness. CIRP Annals – Manufacturing Technology 2016, 65: 281–284, DOI:10.1016/J.CIRP.2016.04.002

7. Zhu X.L., Liu D., Yang Y.H., Yang H. Effects of blank dimension on forming characteristics during conical-section ring rolling of Inco718 alloy, Int. J. Adv. Manuf. Tech. 2016, 84: 2707–2718.

8. Hua, L., Qian, D.S., and Pan, L.B. deformation behaviors and conditions in l-section profile cold ring rolling, Journal of Materials Processing Technology 2009, 209(11): 5087–5096.

9. Qi H., Li Y. Research status and developing trends on the ring rolling process of profile ring parts. Procedia Engineering 2017, 207: 1260–1265.

10. Wei Y.H., Wang Q.D., Zhu Y.P., Zhou H.T., Ding W.J., Chino Y., Mabuchi M. Superplasticity and grain boundary sliding in rolled AZ91 magnesium alloy at high rates. Materials Science & Engineering 2003, 107–115.

11. Luoa X., Li L., Xua W., Zhu Y. Effect of driver roll rotational speed on hot ring rolling of AZ31 magnesium Alloy. Journal of magnesium and alloys 2014, 2: 154–158.

12. Chen X.Q., Guo L.G., Yang H., Zhan M. Study on blank optimization design of conical ring rolling process for TC4 titanium alloy by numerical simulation, J. Plasticity Eng. 2014, 21: 25–31.

13. He H., Yi Y., Huang S., Zhang Y. An improved process for grain refinement of large 2219 Al alloy rings and its influence on mechanical properties. Journal of Materials Science & Technology 2019, 35: 55–63.

14. Qin F.C., Li Y.T., Qi H.P. A casting-rolling compound forming method to produce rings with interior layer of Q345 and external layer of 40Cr. China Invention Patent, No. 201510610375.4.

15. Meier H., Golz J., Hammelmann R. Innovative wear resistant coating by ring rolling: Process integrated powder coating by radial-axial rolling of rings, Ironmak. Steelmak. 2007, 34: 211–215.

16. Kebriaei R., Frischkorn J., Reese S., Husmann S. Numerical modelling of powder metallurgical coatings on ring-shaped parts integrated with ring rolling, J. Mater. Process. Technol. 2013, 213: 2015–2032.

17. He H., Yi Y., Huang S., Zhang Y. An improved process for grain refinement of large 2219 Al alloy rings and its influence on mechanical properties. Journal of Materials Science & Technology 2019, 35: 55–63. DOI:10.1016/j.jmst.2018.09.007.

18. Grosman F., Hadasik E. Technologiczna plastyczność metali. Badania plastometryczne, Gliwice, 2005, (in Polish).

19. Galkin A.M. Badania plastometryczne metali i stopów, Politechnika Częstochowska, Seria Monografie nr 15, Wydawnictwo Politechniki Częstochowskiej, 1990, (in Polish)

20. Kawalek, A., Rapalska-Nowakowska J., Dyja H., Koczurkiewicz B. Physical and numerical modelling of heat treatment the precipitation - Hardening complex - Phase steel (CP). Metalurgija 2013, 52: 23–26.

21. Dyja H., Gałkin A., Knapiński M. Reologia metali odkształcanych plastycznie, seria: Monografie nr 190, Wydawnictwo Politechniki Częstochowskiej, Częstochowa 2010, 220, (in Polish).

22. Danchenko V., Dyja H., Lesik L., Mashkin L., Milenin A. Technologia i modelowanie procesów walcowania w wykrojach, Politechnika Częstochowska, Metalurgia Nr 28, Częstochowa 2002, (in Polish).

23. Arbuz A., Kawałek A., Panichkin A., Ozhmegov K., Popov F., Lutchenko N. Using the radial shear rolling method for fast and deep processing technology of a steel ingot cast structure, Materials, 2023, 16(24).

24. Dembiczak T., Knapiński M., Garbarz B. Mathematical modeling of phenomena of dynamic recrystallization during hot plastic deformation in high-carbon bainitic steel, Metalurgija 2016, 56(1–2): 107–110.

25. Kuvajskova Y.E. Ekonometrika: uchebnoe posobie, UlGTU, Ul'yanovsk 2017, 1–166.

26. Surdacki P., Gontarz A. Analiza porównawcza modeli MES procesu walcowania pierścieni, HUTNIK - Wiadomości hutnicze 2018, 28, (in Polish).

27. Gontarz A., Weroński W.S. Kucie stopów aluminium, WPL, Lublin 2001, (in Polish).